

# NJC

Accepted Manuscript



This is an *Accepted Manuscript*, which has been through the Royal Society of Chemistry peer review process and has been accepted for publication.

*Accepted Manuscripts* are published online shortly after acceptance, before technical editing, formatting and proof reading. Using this free service, authors can make their results available to the community, in citable form, before we publish the edited article. We will replace this *Accepted Manuscript* with the edited and formatted *Advance Article* as soon as it is available.

You can find more information about *Accepted Manuscripts* in the [Information for Authors](#).

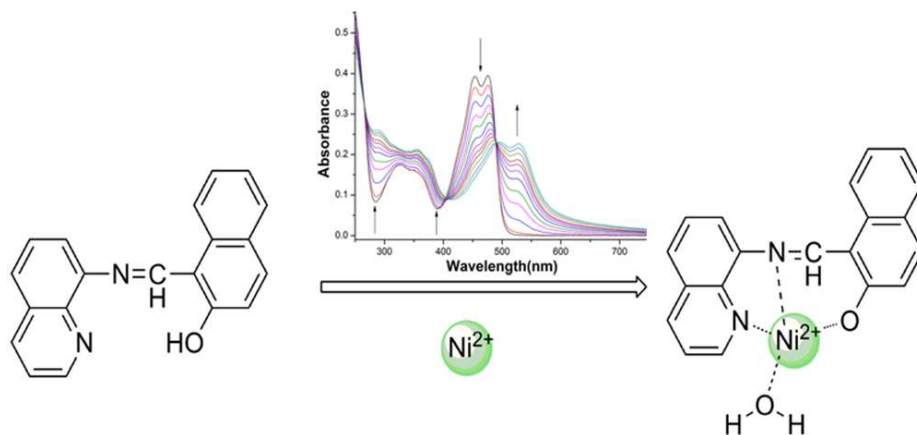
Please note that technical editing may introduce minor changes to the text and/or graphics, which may alter content. The journal's standard [Terms & Conditions](#) and the [Ethical guidelines](#) still apply. In no event shall the Royal Society of Chemistry be held responsible for any errors or omissions in this *Accepted Manuscript* or any consequences arising from the use of any information it contains.



[www.rsc.org/njc](http://www.rsc.org/njc)

## Graphical Abstracts

A highly selective colorimetric chemosensor **LX** was described, which could instantly detect  $\text{Ni}^{2+}$  without interference by other cations.



# **A Highly Selective Colorimetric Chemosensor for Detection of Nickel Ions in Aqueous Solution**

Xin Liu, Qi Lin<sup>\*</sup>, Tai-Bao Wei, You-Ming Zhang<sup>\*</sup>

*Key Laboratory of Eco-Environment-Related Polymer Materials, Ministry of Education of China; Key Laboratory of Polymer Materials of Gansu Province; College of Chemistry and Chemical Engineering, Northwest Normal University, Lanzhou, Gansu, 730070, P. R. China*

---

<sup>\*</sup> Corresponding author. E-mail: linqi2004@126.com (Dr. Q. Lin); zhangwnu@126.com (Prof. Y. M. Zhang)

Tel:+86-931-7973120;

**Abstract**

A highly selective chemosensor **LX** based on quinoline was described, which could instantly detect  $\text{Ni}^{2+}$  in aqueous solution with specific selectivity and high sensitivity. The addition of  $\text{Ni}^{2+}$  to sensor **LX** induced a remarkable color change from yellow to red, these sense procedure could not be interfered by other coexistent competitive cations such as  $\text{Fe}^{3+}$ ,  $\text{Co}^{2+}$ , and  $\text{Cu}^{2+}$ . Thus **LX** could be used as a potential  $\text{Ni}^{2+}$  colorimetric and naked-eye chemosensor. Moreover, test strips based on sensor **LX** were fabricated, which could act as a convenient and efficient  $\text{Ni}^{2+}$  test for “in-the-field” measurement of  $\text{Ni}^{2+}$ .

**Keywords:** Chemosensor; Nickel ions; Naked-eye detection; Ratiometric; Test strips

## 1. Introduction

Nickel is an essential trace element in biological systems such as respiration, biosynthesis, and metabolism [1-3]. Moreover, metallic nickel and its compounds are widely used in modern industry. Nickel compounds are used in electroplating and electroforming and for the production of nickel-cadmium batteries and electronic equipment. Nickel alloys, such as stainless steel, are used in the production of tools, machinery, armaments, and appliances [4-6]. However, the high usage of nickel in such industries inevitably leads to environmental pollution and directly impacts on people's physical health. The accumulation of nickel in the body can lead to lung fibrosis, and cardiovascular and kidney diseases [7-11]. Hence, the rational design and synthesis of efficient sensors to selectively detect  $\text{Ni}^{2+}$  ions at environmental and biological levels are necessary. Up to date, most of  $\text{Ni}^{2+}$ -selective sensors are based on potentiometric methods [12-13]. These sensors also display responses to other transition metal ions, such as  $\text{Co}^{2+}$ ,  $\text{Fe}^{3+}$ ,  $\text{Cu}^{2+}$  and so on [14-18]. According to literatures, only very few reports on detecting  $\text{Ni}^{2+}$  without interference had been published [19-20].

In view of this, and as a part of our research interest in molecular recognition [21-25], we have attempted to obtain an efficient colorimetric and/or fluorescent sensor that could sense  $\text{Ni}^{2+}$  with both high selectivity and sensitivity in aqueous. Our strategy for the design of such a sensor has been as follows. Firstly, colorimetric sensors are promising due to their simplicity, real-time and on-line analysis, especially a significantly lower capital cost than fluorescent sensors. Moreover, paramagnetic  $\text{Ni}^{2+}$  shows the fluorescence quenching nature. So we developed a colorimetric chemosensor that shows a significant color change when binding with  $\text{Ni}^{2+}$ . Secondly, it is well known Schiff base derivatives have been widely used in ion detection for a long time by virtue of their simple structures and good recognition performance, but the detection of  $\text{Ni}^{2+}$  ions based on Schiff base derivatives has rarely been reported. On the other hand, quinoline possess desirable photo-physical properties, they are ideal platforms for development of chemosensors for heavy and transition metal ions.

Therefore, we introduced C=N and quinoline groups into the sensor molecule. Finally, the sensor molecule was designed easy to synthesis. As a result, sensor **LX** could detect Ni<sup>2+</sup> with specific selectivity and high sensitivity in DMSO-H<sub>2</sub>O (v/v=1:1) HEPES buffer solutions at pH=7.4. Moreover, the sense procedure could not be interfered by other coexistent competitive cations (such as Cu<sup>2+</sup>, Fe<sup>3+</sup> and Co<sup>2+</sup>) and anions.

## 2. Experimental

### 2.1. General information and materials

All reagents for synthesis were analytical grade, commercially and were used without further purification. All the cations were added in the form of perchlorate salts and anions were added in the form of tetrabutylammonium (TBA) or sodium salts, which were purchased from Sigma-Aldrich Chemical, stored in a vacuum desiccator. Melting points were measured on an X-4 digital melting point apparatus and were uncorrected. UV/Vis spectra were recorded on a Shimadzu UV-2550 spectrometer at room temperature. <sup>1</sup>H NMR spectra were recorded on a Varian Mercury Plus-400 MHz spectrometer with DMSO-*d*<sub>6</sub> as solvent and TMS as an internal reference. The infrared spectra were performed on a Digilab FTS-3000 FT-IR spectrophotometer. Elemental analyses were performed by Thermo Scientific Flash 2000 organic elemental analyzer.

### 2.2. General procedure for UV-vis experiments

Stock solutions of  $4.0 \times 10^{-3} \text{ mol} \cdot \text{L}^{-1}$  perchlorate salts of the respective cations (Fe<sup>3+</sup>, Ag<sup>+</sup>, Ca<sup>2+</sup>, Cu<sup>2+</sup>, Co<sup>2+</sup>, Ni<sup>2+</sup>, Cd<sup>2+</sup>, Pb<sup>2+</sup>, Zn<sup>2+</sup>, Cr<sup>3+</sup>, and Mg<sup>2+</sup>) and  $1.0 \times 10^{-2} \text{ mol} \cdot \text{L}^{-1}$  tetrabutylammonium or sodium salts of the respective anions (F<sup>-</sup>, Cl<sup>-</sup>, Br<sup>-</sup>, I<sup>-</sup>, AcO<sup>-</sup>, H<sub>2</sub>PO<sub>4</sub><sup>-</sup>, HSO<sub>4</sub><sup>-</sup>, ClO<sub>4</sub><sup>-</sup> and CN<sup>-</sup>) were prepared in water. A stock solution of sensor **LX** ( $2.0 \times 10^{-4} \text{ mol} \cdot \text{L}^{-1}$ ) was prepared in DMSO. The solution of sensor **LX** was then diluted to  $2.0 \times 10^{-5} \text{ mol} \cdot \text{L}^{-1}$  with DMSO-H<sub>2</sub>O (v/v=1:1, pH=7.4) HEPES buffer solutions. In titration experiments, 2 mL solution of sensor **LX** ( $2.0 \times 10^{-5} \text{ mol} \cdot \text{L}^{-1}$ ) was filled in a quartz optical cell of 1 cm optical path length, and the ions stock solution were added into the quartz optical cell gradually by using a micropipet. Spectral data were recorded at 10 min after addition of the ions at room temperature.

### 2.3. General procedure for $^1\text{H}$ NMR experiments

For  $^1\text{H}$  NMR titration, sensor **LX** was prepared in  $\text{DMSO-}d_6$ ,  $\text{Ni}(\text{ClO}_4)_2$  was prepared in  $\text{D}_2\text{O}$ . First of all, only sensor **LX** in  $\text{DMSO-}d_6$  were added into NMR tube, and then added  $\text{Ni}^{2+}$  ions at 0.5, 1.0 and 1.5 equiv sequentially. All solutions were mixed directly in NMR tube.

### 2.4. Synthesis of the sensor **LX**

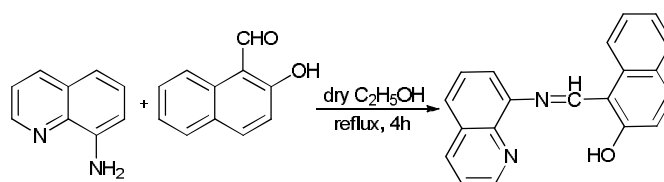
The structure and synthesis of sensor **LX** is shown in Scheme 1. 8-aminoquinoline (0.29 g, 2 mmol), 2-hydroxy-1-naphthaldehyde (0.35 g, 2 mmol) in dry ethanol (30 mL) was stirred under reflux condition for 4 h, and get yellow product (0.51 g, 85% yield) after recrystallization from  $\text{C}_2\text{H}_5\text{OH-DMF}$ .

m.p. 227-229°C. IR (KBr,  $\text{cm}^{-1}$ ):  $\nu = 3447(\text{OH})$ ,  $1624(\text{C}=\text{N})$ ,  $1589(\text{C}=\text{N})$ ,  $1535(\text{C}=\text{C})$ .  $^1\text{H}$  NMR (400 MHz, DMSO)  $\delta$  15.91 (d,  $J = 10.8$  Hz, 1H, OH), 9.66-9.51 (m, 1H, =CH), 9.05 (dd,  $J = 4.1, 1.7$  Hz, 1H), 8.47 (dd,  $J = 14.9, 4.8$  Hz, 3H), 7.91-7.16 (m, 7H, Ar-H), 6.72 (dd,  $J = 9.5, 5.8$  Hz, 1H).  $^{13}\text{C}$  NMR (151 MHz, DMSO)  $\delta$  181.42 (s), 150.17 (s), 147.25 (s), 139.38 (s), 138.74 (s), 136.45 (s), 136.26 (s), 134.24 (s), 129.12 (s), 128.39 (d,  $J = 6.4$  Hz), 126.96 (s), 126.29 (s), 125.92 (s), 124.44 (s), 123.46 (s), 122.59 (s), 119.93 (s), 114.63 (s), 108.24 (s). Anal. calcd for  $\text{C}_{20}\text{H}_{14}\text{N}_2\text{O}$ : C 80.52, H 4.73, N 9.39; found: C 80.60, H 4.58, N 9.37. ESI-MS: calcd for  $[\text{C}_{20}\text{H}_{14}\text{N}_2\text{O}+\text{H}]^+$  299.1, found 299.3.

### 2.5. Synthesis of the **LX-Ni**

The DMF solution of **LX** (0.030 g, 0.1mmol) and the water solution of  $\text{Ni}(\text{ClO}_4)_2 \cdot 6\text{H}_2\text{O}$  (0.055 g, 0.15mmol) were mixed and stirred at room temperature for 2 h. The red solid formed was filtered, washed with water and dried under vacuum.

m.p. 262-264°C. IR (KBr,  $\text{cm}^{-1}$ ):  $\nu = 3441(\text{OH})$ ,  $1614(\text{C}=\text{N})$ ,  $1534(\text{C}=\text{C})$ ,  $1492(\text{C}=\text{C})$ . ESI-MS: calcd for  $[\text{LX}+\text{Ni}^{2+}+\text{H}_2\text{O}]^+$  373.1, found 373.3.



**Scheme 1.** Structure and synthesis of the sensor **LX**.

### 3. Results and discussion

The sensing abilities of **LX** toward various cations ( $\text{Fe}^{3+}$ ,  $\text{Ag}^+$ ,  $\text{Ca}^{2+}$ ,  $\text{Cu}^{2+}$ ,  $\text{Co}^{2+}$ ,  $\text{Ni}^{2+}$ ,  $\text{Cd}^{2+}$ ,  $\text{Pb}^{2+}$ ,  $\text{Zn}^{2+}$ ,  $\text{Cr}^{3+}$ , and  $\text{Mg}^{2+}$ ) were investigated by UV-vis spectroscopy. When 10 equivalents of these cations ( $c=2\times 10^{-4}$  M) was added to the DMSO- $\text{H}_2\text{O}$  ( $v/v=1:1$ ,  $\text{pH}=7.4$ ) HEPES buffer solutions of sensor **LX** ( $c=2\times 10^{-5}$  M) respectively at room temperature, a dramatic color change from yellow to red was observed by the naked-eye only upon the addition of  $\text{Ni}^{2+}$  to sensor **LX** (Figure 1). In the corresponding UV-vis spectra (Figure 2), the formation of a new absorption band at about 525 nm is in good agreement with this color change. All examined cations such as  $\text{Fe}^{3+}$ ,  $\text{Co}^{2+}$  and  $\text{Cu}^{2+}$  didn't cause any obvious color and spectra changes. The plot of changes in the absorbance at 525 nm upon addition of various cations clearly showed excellent selectivity of sensor **LX** towards the  $\text{Ni}^{2+}$  (Figure 3). Moreover, we also explored the optical response of sensor **LX** by monitoring the changes in absorption spectra upon addition of various anions ( $\text{F}^-$ ,  $\text{Cl}^-$ ,  $\text{Br}^-$ ,  $\text{I}^-$ ,  $\text{AcO}^-$ ,  $\text{H}_2\text{PO}_4^-$ ,  $\text{HSO}_4^-$ ,  $\text{ClO}_4^-$  and  $\text{CN}^-$ ) under the same conditions, no obvious color and spectra changes were observed (Supporting Information, Figure S1).



Figure 1. Color changes of **LX** ( $c=2\times 10^{-5}$  M) after addition of 10 equivalents various cations in DMSO- $\text{H}_2\text{O}$  ( $v/v=1:1$ ) HEPES buffer solutions at  $\text{pH}=7.4$ . From left to right: only **LX**,  $\text{Fe}^{3+}$ ,  $\text{Ag}^+$ ,  $\text{Ca}^{2+}$ ,  $\text{Cu}^{2+}$ ,  $\text{Co}^{2+}$ ,  $\text{Ni}^{2+}$ ,  $\text{Cd}^{2+}$ ,  $\text{Pb}^{2+}$ ,  $\text{Zn}^{2+}$ ,  $\text{Cr}^{3+}$ ,  $\text{Mg}^{2+}$ .

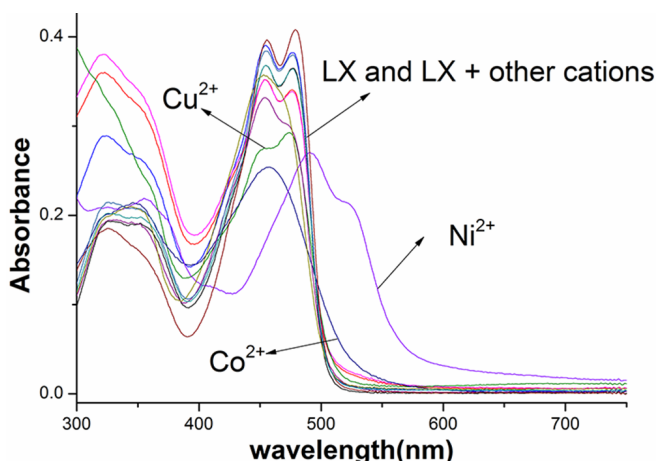


Figure 2. Changes in the UV/Vis spectra of **LX** ( $c=2\times 10^{-5}$  M) after addition of 10 equivalents various cations in DMSO- $H_2O$  ( $v/v=1:1$ ) HEPES buffer solutions at  $pH=7.4$ .

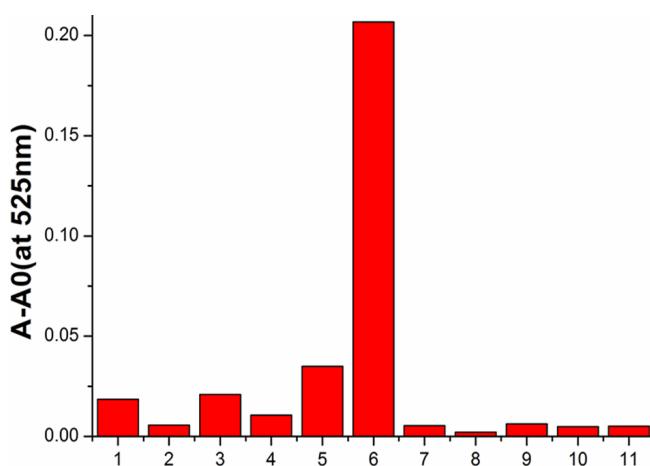


Figure 3. Normalized changes in the absorbance at 525 nm of **LX** ( $c=2\times 10^{-5}$  M) after addition of 10 equivalents various cations, from 1 to 11:  $Fe^{3+}$ ,  $Ag^+$ ,  $Ca^{2+}$ ,  $Cu^{2+}$ ,  $Co^{2+}$ ,  $Ni^{2+}$ ,  $Cd^{2+}$ ,  $Pb^{2+}$ ,  $Zn^{2+}$ ,  $Cr^{3+}$ ,  $Mg^{2+}$ .

Figure 4 shows the family of absorption spectra obtained over the course of the titration of sensor **LX** with  $Ni^{2+}$  in DMSO- $H_2O$  ( $v/v=1:1$ ) HEPES buffer solutions at  $pH=7.4$ . With the gradual addition of pure water solution of  $Ni^{2+}$  to sensor **LX**, the intensity of absorption bands at 525 nm, 389 nm and 284 nm increased, while an absorption bands at 464 nm began to decrease until it reached a limiting value. Moreover the presence of three isosbestic points at 490, 265 and 405 nm indicated that sensor **LX** reacts with  $Ni^{2+}$  to form a stable complex. Simultaneously, the ratio of  $A_{525}/A_{464}$  rises along with the increase in  $Ni^{2+}$  concentrations, which allows the  $Ni^{2+}$  concentration to be determined ratiometrically (Supporting Information, Figure S2). From titration plots in UV-visible spectroscopy, the 1:1 stoichiometry between  $Ni^{2+}$

and sensor **LX** has been proved.

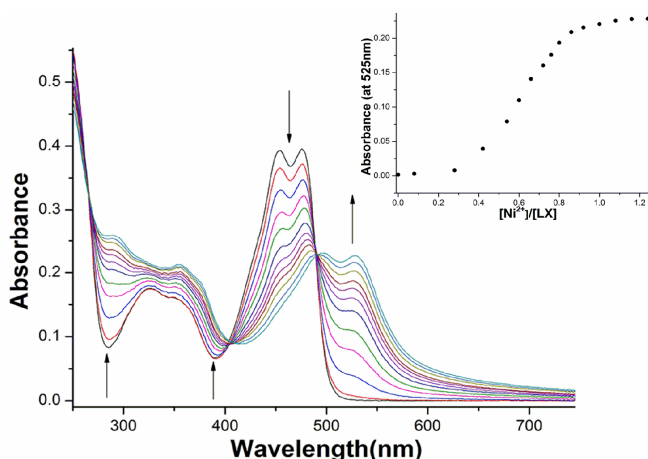


Figure 4. UV-vis spectra of **LX** ( $c=20\ \mu\text{M}$ ) upon the addition of  $\text{Ni}^{2+}$ .  $[\text{Ni}^{2+}] = 0, 5.6, 8.4, 10.8, 12.0, 13.2, 14.4, 15.2, 16.4, 18.4, 20.0, 21.6\ \mu\text{M}$ . Inset: plot of absorbance at 525 nm vs. number of equivalents of  $\text{Ni}^{2+}$ .

To know stoichiometry between the guest ( $\text{Ni}^{2+}$ ) and host **LX** molecule in DMSO- $\text{H}_2\text{O}$  ( $v/v=1:1$ ) HEPES buffer solutions at  $\text{pH}=7.4$ . Job's plot has been drawn (Figure 5). When molar fraction of  $\text{Ni}^{2+}$  was 0.5, the absorbance at 525 nm got to extreme value, indicating that forming a 1:1 complex between **LX** and  $\text{Ni}^{2+}$ . The association constant ( $K_a$ ) of **LX** with  $\text{Ni}^{2+}$  was determined using the Benesi-Hildebrand equation [26-28]. The measured absorbance  $[1/(A-A_0)]$  varied as a function of  $1/[\text{Ni}^{2+}]$  in a linear relationship ( $R=0.9887$ ), indicating formation of 1:1 stoichiometry between  $\text{Ni}^{2+}$  and **LX**. This conclusion is consistent with corresponding Job's plot. The association constant of **LX** with  $\text{Ni}^{2+}$  in DMSO- $\text{H}_2\text{O}$  ( $v/v=1:1$ ) HEPES buffer solutions at  $\text{pH}=7.4$  was calculated to be  $1.33 \times 10^5\ \text{M}^{-1}$  (Supporting Information, Figure S3).

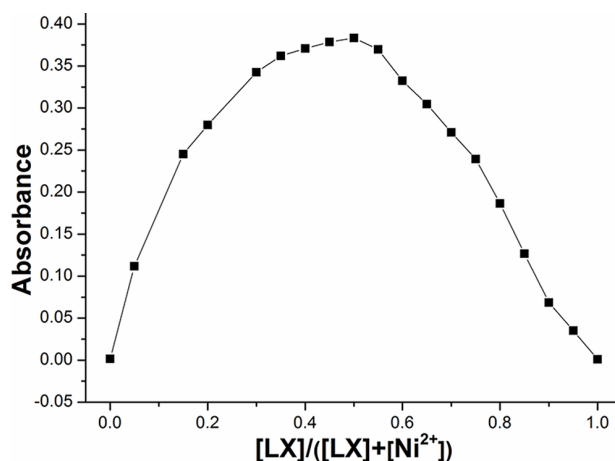


Figure 5. Jobs plot for complexation of sensor **LX** with  $\text{Ni}^{2+}$  in DMSO- $\text{H}_2\text{O}$  (v/v=1:1) HEPES buffer solutions at pH=7.4.

As known, chemosensors always have a problem of long response time. In our case, the binding process of  $\text{Ni}^{2+}$  to **LX** was found to be very fast (Figure 6). After adding  $\text{Ni}^{2+}$ , the absorbance of **LX** was increased at 525 nm and reached the plateau region less than 12 s, and remains quite stable, suggesting that the binding process might be completed instantly and the chemosensor has rapid detection ability for nickel cation.

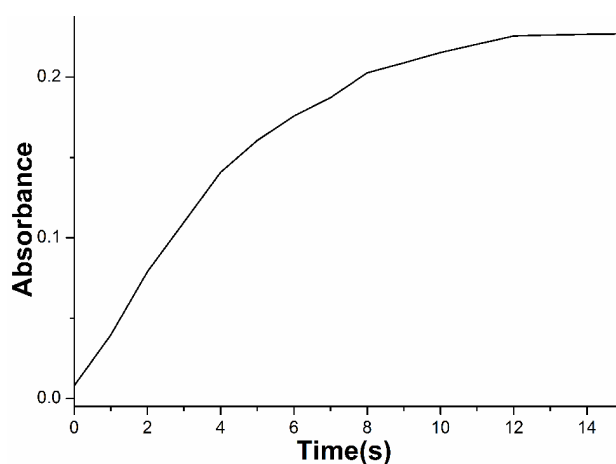


Figure 6. The time-dependent absorbance at 525 nm for **LX** ( $2.0 \times 10^{-5}$  M) in DMSO- $\text{H}_2\text{O}$  (v/v=1:1) HEPES buffer solutions at pH=7.4 after addition of 10 equivalents  $\text{Ni}^{2+}$ .

An important feature of a sensor is its selectivity toward analyze relative to other competitive species. Therefore, competition experiments were carried out by adding  $\text{Ni}^{2+}$  ions ( $c=2 \times 10^{-4}$  M) to solution of **LX** ( $c=2 \times 10^{-5}$  M) in the presence of miscellaneous ions including anions ( $c=1 \times 10^{-3}$  M) and cations ( $c=2 \times 10^{-4}$  M), respectively. These miscellaneous competitive ions did not induce significant absorption changes of **LX** in the absence of  $\text{Ni}^{2+}$ . However, upon addition of  $\text{Ni}^{2+}$  to the solution, the unique spectral and color changes were still displayed under the above conditions (Figure 7&8). These results revealed that **LX** had a remarkable selectivity toward  $\text{Ni}^{2+}$  over other competitive ions, and more, the detection of  $\text{Ni}^{2+}$  by **LX** was hardly affected by these common coexistent cations and anions.

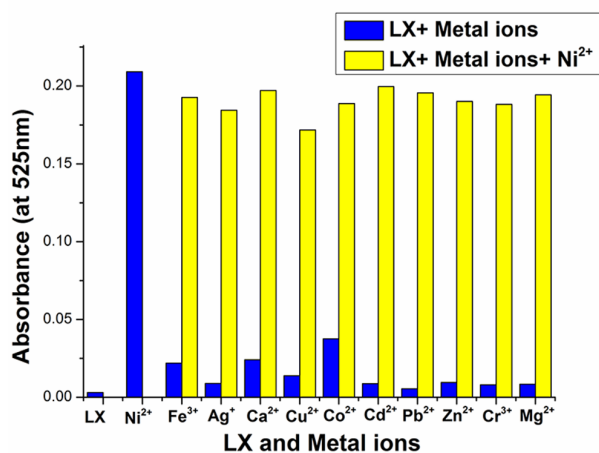


Figure 7. Absorbance responses of LX ( $c=2\times 10^{-5}$  M) in the presence of 10 equivalents Ni<sup>2+</sup> with 10 equivalents various metal ions in DMSO-H<sub>2</sub>O (v/v=1:1) HEPES buffer solutions at pH=7.4. Bars represent absorbance at 525 nm. The blue bars represent the addition of the competing metal ions to solution of LX. The yellow bars represent the addition of competing metal ions and Ni<sup>2+</sup> to the solution of LX.

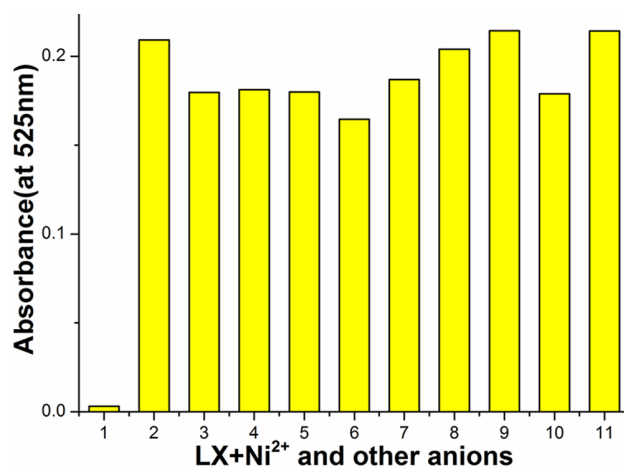


Figure 8. Absorbance at 525 nm of LX ( $c=2\times 10^{-5}$  M) in the presence 10 equivalents Ni<sup>2+</sup> with 50 equivalents various anions in DMSO-H<sub>2</sub>O (v/v=1:1) HEPES buffer solutions at pH=7.4. From 1 to 11: LX, LX+Ni<sup>2+</sup>, LX+Ni<sup>2+</sup>+F<sup>-</sup>, LX+Ni<sup>2+</sup>+Cl<sup>-</sup>, LX+Ni<sup>2+</sup>+Br<sup>-</sup>, LX+Ni<sup>2+</sup>+I<sup>-</sup>, LX+Ni<sup>2+</sup>+AcO<sup>-</sup>, LX+Ni<sup>2+</sup>+H<sub>2</sub>PO<sub>4</sub><sup>-</sup>, LX+Ni<sup>2+</sup>+HSO<sub>4</sub><sup>-</sup>, LX+Ni<sup>2+</sup>+ClO<sub>4</sub><sup>-</sup>, LX+Ni<sup>2+</sup>+CN<sup>-</sup>.

The colorimetric detection limits of sensor LX for Ni<sup>2+</sup> were also tested. As is shown in Figure 9, the minimum concentration of Ni<sup>2+</sup> for color change observed by the naked-eye was  $5.0\times 10^{-6}$  M and the detection limit of the absorption spectra changes calculated on the basis of  $3s_B/S$  [29] was  $2.2\times 10^{-7}$  M for Ni<sup>2+</sup> cation (Supporting Information, Figure S4).



Figure 9. Naked-eye detection limit.

Motivated by the favorable features of sensor **LX** in solution, we prepared test strips by immersing filter papers ( $3 \times 1 \text{ cm}^2$ ) into the DMSO solution of sensor **LX** ( $1 \times 10^{-3} \text{ M}$ ) and then dried them in air to determine the suitability of a “dip-stick” method for the detection of  $\text{Ni}^{2+}$ , similar to that commonly used for the pH measurement. When the test strips coated with **LX** ( $1 \times 10^{-3} \text{ M}$ ) were immersed into the pure water solutions of  $\text{Ni}^{2+}$  with different concentrations, the obvious color change from yellow to red was observed (Figure 10). The development of such a “dip-sticks” approach was extremely attractive for “in-the-field” measurements that did not require any additional equipment. Therefore, the test strips of **LX** have excellent application value in detection  $\text{Ni}^{2+}$ .

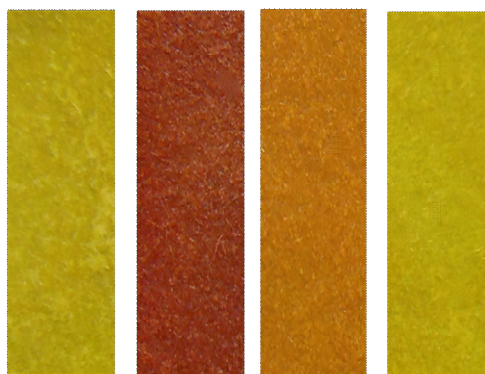


Figure 10. Color change of the test strips of **LX** ( $1 \times 10^{-3} \text{ M}$ ) to various concentrations of  $\text{Ni}^{2+}$  in water, from left to right: 0,  $1 \times 10^{-3} \text{ M}$ ,  $1 \times 10^{-4} \text{ M}$ , and  $1 \times 10^{-5} \text{ M}$ .

To explore the sensing mechanism of sensor **LX** to  $\text{Ni}^{2+}$ , the IR,  $^1\text{H}$  NMR titration and ESI-MS were investigated, which illustrated the characteristic structural changes occurring upon interaction with  $\text{Ni}^{2+}$ . In the IR spectra of **LX**, the stretching

vibration absorption peaks of HC=N, quinoline C=N appeared at  $1624\text{ cm}^{-1}$ ,  $1591\text{ cm}^{-1}$  and in plane bending vibration absorption peak of O-H at  $1301\text{ cm}^{-1}$ , respectively. However, when **LX** coordinated with  $\text{Ni}^{2+}$ , the stretching vibration absorption peaks of HC=N and in plane bending vibration absorption peak of O-H disappeared, meanwhile the stretching vibration absorption peak of quinoline C=N shifted to higher wavenumbers at  $1614\text{ cm}^{-1}$  (Figure 11). These changes indicated that nickel ions had coordination with imine nitrogen atoms, oxygen atoms of phenolic hydroxyl groups and nitrogen atoms of quinoline of **LX**, respectively (Scheme 2).

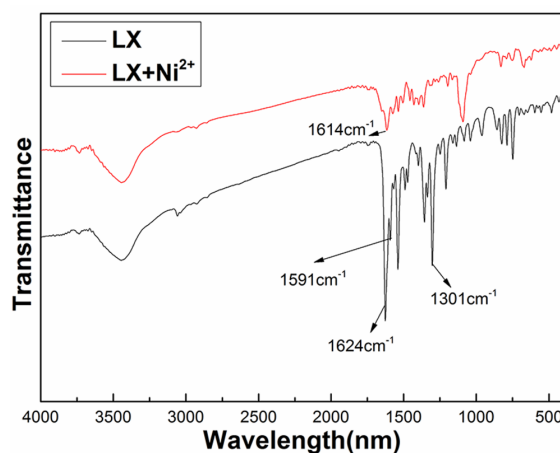
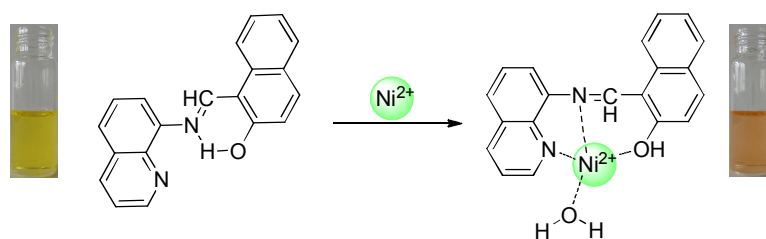


Figure 11. IR spectra of compound **LX** and **LX-Ni<sup>2+</sup>** in KBr disks.



Scheme 2. A possible sense mechanism of the sensor **LX** to  $\text{Ni}^{2+}$ .

The results of  $^1\text{H}$  NMR experiments also support this proposed mechanism (Supporting Information, Figure S5). There is one intramolecular hydrogen bond in the molecular structure of **LX**:  $\text{OH}\cdots\text{N}=\text{C}$ . The formation of this strong hydrogen bond leads to the  $^1\text{H}$  NMR chemical shift the OH group appearing at very low-field, 15.9 ppm. With gradual addition of  $\text{Ni}^{2+}$ , the OH peak at 15.9 ppm shifted to 11.4 ppm and became broad, which can be attributed to the breaking of intramolecular hydrogen bond by  $\text{Ni}^{2+}\cdots\text{O-H}$  interactions. Meanwhile, the signal of the hydrogen atoms in

aromatic rings and CH=N showed a significant downfield shift, indicating a charge transfer from aromatic groups to the Ni<sup>2+</sup> ions. These results also suggested that Ni<sup>2+</sup>-LX complex was formed via the coordination of Ni<sup>2+</sup> with OH, C=N and nitrogen atoms of quinoline on LX.

Further evidence was obtained by ESI-MS experiments also support this proposed mechanism. In the ESI-MS spectra of sensor LX (Figure S6), the [LX+H]<sup>+</sup> peak appeared at 299.3 (m/z<sub>calcd</sub>=299.1). However, when 1 equivalent Ni<sup>2+</sup> was added to the solution of LX, a new peak appeared at 373.3, coinciding well with that for the species [LX+H<sub>2</sub>O+Ni<sup>2+</sup>]<sup>+</sup> (m/z<sub>calcd</sub>=373.1) and indicating the formation of the stabilized cationic species LX-Ni<sup>2+</sup> (Figure S7).

#### 4. Conclusion

In summary, we have developed a Ni<sup>2+</sup> sensor, which could detect Ni<sup>2+</sup> in aqueous solution with specific selectivity and high sensitivity in a very short time. A unique colorimetric response to Ni<sup>2+</sup> is realized through the coordination with sensor LX. In particular, competitive cations such as Fe<sup>3+</sup>, Co<sup>2+</sup> and Cu<sup>2+</sup> did not afford any obvious interference response. The detection limits were 5.0×10<sup>-6</sup> M and 2.2×10<sup>-7</sup> M of Ni<sup>2+</sup> using the naked-eye color changes and absorption spectra changes respectively. Moreover, test strips based on sensor LX was fabricated, which could serve as practical colorimetric sensor for “in-the-field” measurement of Ni<sup>2+</sup> and did not require any additional equipment but just by virtue of “dip-sticks” approach. We believe the test strips could act as a convenient and efficient Ni<sup>2+</sup> test kit.

#### Acknowledgment

This work was supported by the National Natural Science Foundation of China (NSFC) (Nos. 21064006; 21161018; 21262032), the Natural Science Foundation of Gansu Province (1308RJZA221) and the Program for Changjiang Scholars and innovative Research Team in University of Ministry of Education of China (IRT1177).

#### References

- [1] S.B. Mulrooney, R.P. Hausinger, *Microbiol. Rev.* 2003, **27**, 239.
- [2] S.W. Ragsdale, *J. Biol. Chem.* 2009, **284**, 18571.

- [3] R.J. Maier, *Biochem. Soc. Trans.* 2005, **33**, 83.
- [4] K.S. Kasprzak, F.W. Sunderman, K. Salnikowa, *Mutat Res.* 2003, **533**, 67.
- [5] P.H. Kuck, *Mineral Commodity Summaries 2006: Nickel*, United States Geological Survey.
- [6] J.R. Davis, *Uses of Nickel*, ASM Specialty Handbook: Nickel, Cobalt, and Their Alloys. *ASM International*, 2000. 7.
- [7] E. Denkhaus, K. Salnikow, *Crit. Rev. Oncol. Hematol.* 2002, **42**, 35.
- [8] X.Q. Liu, X. Zhou, X. Shu, J. Zhu, *Macromolecules.* 2009, **42**, 7634.
- [9] J.R. Sheng, F. Feng, Y. Qiang, F.G. Liang, L. Sen, F.H. Wei, *Anal. Lett.* 2008, **41**, 2203.
- [10] H.X. Wang, D.L. Wang, Q. Wang, X.Y. Li, C.A. Schalley, *Org. Biomol. Chem.* 2010, **8**, 1017.
- [11] L. Feng, Y. Zhang, L.Y. Wen, L. Chen, Z. Shen, Y. F. Guan, *Analyst* 2011, **136**, 4197.
- [12] M. Shamsipur, T. Poursaberi, A.R. Karami, M. Hosseini, A. Momeni, N. Alizadeh, *Anal. Chim. Acta.* 2004, **501**, 55.
- [13] V.K. Gupta, R.N. Goyal, S. Agarwal, P. Kumar, N. Bachheti, *Talanta* 2007, **71**, 795.
- [14] I. Grabchev, J.M. Chovelon, X. Qian, *New J. Chem.* 2003, **27**, 337.
- [15] H.Q. Li, L. Cai, J.X. Li, Y.X. Hu, P.P. Zhou, J.M. Zhang, *Dyes Pigments.* 2011, **91**, 309.
- [16] C. Ma, A. Lo, A. Abdolmaleki, M.J. MacLachlan, *Org. Lett.* 2004, **6**, 3841.
- [17] I. Grabchev, J.M. Chovelon, A. Nedelcheva, *J. Photochem. Photobiol A: Chem.* 2006, **183**, 9.
- [18] I. Qureshia, M.A. Qazia, S. Memon, *Sens. Actuators B.* 2009, **141**, 45.
- [19] H. Li, S.J. Zhang, C.L. Gong, Y.F. Li, Y. Liang, Z.G. Qi, S. Chen, *Analyst.* 2013, **138**, 7090.
- [20] S. Goswami, S. Chakraborty, S. Paul, S. Halder, A.C. Maity, *Tetrahedron Letters* 2013, **54**, 5075.
- [21] Q. Lin, X. Liu, T.B. Wei, Y.M. Zhang, *Chem. Asian J.* 2013, **8**, 3015.

- [22] Q. Lin, Y.P. Fu, P. Chen, T.B. Wei, Y.M. Zhang, *Dyes Pigments*. 2013, **96**, 1.
- [23] Y.M. Zhang, Q. Lin, T.B. Wei, Y. Li, X.P. Qin, *Chem. Commun.* 2009, **45**, 6074.
- [24] B.B. Shi, P. Zhang, T.B. Wei, H. Yao, Q. Lin, Y.M. Zhang, *Chem. Commun.* 2013, **49**, 7812.
- [25] Q. Lin, X. Liu, T.B. Wei, Y.M. Zhang, *Sens. Actuators B*. 2014, **190**, 459.
- [26] Y. Xie, Y. Ding, X. Li, C. Wang, J.P. Hill, K. Ariga, W. Zhang, W. Zhu, *Chem. Commun.* 2012, **48**, 11513.
- [27] Y. Ding, X. Li, T. Li, W. Zhu, Y. Xie, *J. Org. Chem.* 2013, **78**, 5328.
- [28] B. Chen, Y. Ding, X. Li, W. Zhu, J.P. Hill, K. Ariga, Y. Xie, *Chem. Commun.* 2013, **49**, 10136.
- [29] Analytical Methods Committee, *Analyst*. 1987, **112**, 199.